Preferred citation: M. Mikczinski, H.X. Nguyen and S. Fatikow. Assessing transverse fibre properties: fibre compression and artificial hornification by periodic compression. In **Advances in Pulp and Paper Research, Cambridge 2013**, *Trans. of the XVth Fund. Res. Symp. Cambridge, 2013*, (S.J. I'Anson, ed.), pp 803–820, FRC, Manchester, 2018. DOI: 10.15376/frc.2013.2.803.

ASSESSING TRANSVERSE FIBRE PROPERTIES: FIBRE COMPRESSION AND ARTIFICIAL HORNIFICATION BY PERIODIC COMPRESSION

Manuel Mikczinski[1], Ha Xuan Nguyen[2], and Sergej Fatikow[1,2]*

[1] OFFIS – Institute for Information Technology, Division Health, Group Automated Nanohandling, Escherweg 2, D-26121 Oldenburg, Germany
[2] University of Oldenburg, Division Microrobotics and Control Engineering, D-26111 Oldenburg, Germany

May 24, 2013

ABSTRACT

Assessing material properties on the micro and nanoscale requires appropriate tools and measurement systems. Micro- and nanorobotic systems allow for such investigations. This contribution represents a case study in this respect. A setup capable of compressing single fibres with force feedback under scanning electron microscopy observation is presented and used. Variations in the compression force during testing of single fibres are reported and analysed. It is shown that significant alterations of the fibre wall mechanical properties are already introduced during testing one fibre several times in the transverse direction. Although hornification is generally used in the context of changes on the fibre wall due to drying and rewetting cycles of fibres or paper, it is suggested to expand the term also on changes induced by mechanical treatment, as the outcome could be similar.

* Author to whom correspondence should be addressed: manuel.mikczinski@unioldenburg.de

Furthermore, a microrobotic method and a system are proposed which will allow simulating the mechanical hornification and which are based on a force generating apparatus.

1 INTRODUCTION

Mechanical properties of single fibres and paper have been of interest ever since papermaking was industrialised. Since the first experiments on single fibre mechanical properties were made by Jayne [9] there was lots of progress in single fibre testing. A recent overview by Eder and co-workers [6] sums up the work and also mentions the future challenge: measuring mechanical fibre properties in all fibre directions. So far, mostly the longitudinal fibre direction is assessed [9, 14, 11, 2] by micro-tensile test equipment. However, single fibres are also assessed by other means, like indentation. Prominent examples are the fibre surface indentation with an atomic force microscope (AFM) tip, e.g. most recently by [19], and a prepared pillar structure in the S2 layer of the fibre is compressed in a wood specimen, e.g. [20, 1].

Cyclic loading of single fibres was also presented earlier by Wild and coworkers [18]. Nowadays the dynamic mechanical analysis (DMA) of single fibres is a useful tool to obtain its visco-elastic properties. These techniques stress the fibres in the longitudinal direction. Often the fibres are glued to frame-like sample holders similar to the ones presented already by Page and co-workers [14] and more recently by Burgert *et al.* [2] for tensile testing.

Due to the advancements in robotics and testing equipment mechanical properties of single fibres are nowadays easier assessable. However, there is still a gap from single fibre measurements to the cell wall level measurements made by AFM. In the first type of measurements the whole fibre is manipulated. In the latter type, only small features of the cell wall are treated. Hence, for fibre-level sized features new methods and systems need to be realised.

Regarding the effects on the stiffness of the fibre due to periodical mechanical loading, hornification might be one expression. Hornification could be understood as the crosslinking of the fibrillar structure [8, 7]. However, also other effects, especially chemical reactions, e.g. hydrogen bonding [10] or lactone [7], are thought to influence the hornification of fibres. In any case includes the term hornification mechanical, structural, and chemical aspects and is focusing on the fibre's response on drying and rewetting.

The need to understand in more detail the structure of cellulose and the structures it forms throughout the different scales (CNC, NFC, MFC, fibres, films, paper, and board) became more urgent in the last decade due to rising costs of raw material and energy. Discussing sustainability increased the awareness even more. However, the understanding what happens on the different smaller scales (nano, micro, meso) is still not sufficient. More recent technical advancements in the robotics area closes this gap of single fibre treatment and characterisation [16, 12] and allows localised testing of individual fibre features. Thanks to automation of the micro- and nanorobotic systems even statistical relevant data are in reach. By increasing the dexterity of these systems also transverse fibre properties are possible.

The following section will introduce microrobotic systems to (i) measure the force during a compression cycle in the μ to mN range and (ii) to generate a periodic compression force on a target. These tools are affecting only a part of the fibre and not the whole fibre. Two pine fibres (*Pinus silvestris*) will be tested on compression. Furthermore, two virgin spruce fibres (*Picea abies* [L.] Karst.) are tested prior and after they are periodically compressed with the force generation device, described in Section 2. The results of these measurements are presented in Section 3 and discussed in Section 4. Section 5 will conclude on the results and propose future developments in terms of testing methods and systems as well as interpretation of results.

2 SYSTEMS AND METHODS

This section presents the sample preparation and the microrobotic system to perform the compression measurement. Furthermore, in the end of this section another microrobotic system is described which is suitable to compress the fibres with a pre-set force for a pre-defined number of cycles. Therewith, a mechanical pressing influence on the fibres can be simulated.

2.1 Sample Preparation

As specimens two different fibre types are used. On the one hand bleached softwood kraft pulp from pine (*Pinus silvestris*, STORA 32) was used for the compressibility experiments. These fibres were provided as dry-lap sheets from the manufacturer without any further treatment. On the other hand adult earlywood fibres from spruce (*Picea abies* [L.] Karst.) were used for the periodic compression experiments. Those were carefully extracted with tweezers as described with Burgert *et al.* [3] and Olsson *et al.* [13]. The earlywood spruce fibres were provided as single fibres floating in de-ionised water.

For the compressibility measurement, a small amount of pine fibres (ca. 10 . . . 14 mg) is ripped from the dry-lap sheet with tweezers and put in micro test tubes (Eppendorf, 1.5 ml). Approximately 1 ml Millipore is added and the tubes are shaken with ca. 1200 rpm at 25°C for ca. eight hours until most of the fibres are separated. Afterwards the resulting lumps are put in a petri dish with Millipore and further separated with tweezers. From there four single fibres are taken and dried at air in the microscope light. They are placed on a cutting mat and cut with a fresh razor blade. The remaining four fibre halves are placed on the modified SEM stub, which is described below.

For the periodic compression experiments, two earlywood adult spruce fibres are taken from the water with tweezers, cut with a fresh razor blade, and placed on the specifically modified SEM stub (12.5*mm* diameter, G301F, Plano, Germany), see also top right corner of Figure 1. Therefore, they are henceforth labeled halves with Spruce 1 and 2, and a and b denote the corresponding halfs of the fibres.

On this stub two tiles of silicon (5 *mm* × 5 *mm*, G3388, Plano, Germany) are fixed with two-component adhesive to form a perfect flat background for the compression testing. The stub is then coated with layer of ca. 10 *nm* gold to facilitate the electron transport when visualised in SEM. Additionally, half a sticky carbon pad (PELCO Tabs™, 16084-1, Ted Pella Inc., USA) is placed below the silicon tiles.

The fibres are in both cases fixed on the sticky pad so that the part of the fibre, which will be tested, is free-standing over the silicon tiles. The complete sample holder and the samples are not coated, as the experiments are performed in a FEI Quanta 600 SEM with low vacuum mode (0.8 . . . 1 *mbar*). Therewith, the influence on the mechanical properties are kept to a minimum.

2.2 Microrobotic Compression Measurement Setup

As micro-/nanorobotic manipulation system the PS-AMiR is used. Firstly presented in [12] this collection of modules evolved and is used to assemble customised systems for all sorts of fibre manipulations inside or outside the SEM. The modular system consists of a base plate carrying the different modules either in a centre position or in a perimeter position facing the centre point. Various modules are currently available. For this compression testing one coarse (perimeter) and one fine positioning (centre) module were chosen, see Figure 1. On the centre module a XY nano-positioning unit with a stroke of 50 *μm* and subnanometre resolution (Physik Instrumente, Germany) performed the measurement movement and carried the sample. The stub is tilted by 90º to allow the visualisation of the fibre cross-section during testing. On the perimeter module a XYZ micro-positioning system with a travel of ca. 12 *mm* with sub-micron resolution (SmarAct GmbH, Germany) is used to position the force sensor as close as possible to the fibre. A capacitive force sensor, FT-S270 (Femtotools, Switzerland) with a measurement range of ±1*mN* and a resolution of ideally 0.4 *N* was used. The sensor tip is flat with a size of 50 *μm* × 50 *μm*. During testing the sensor was sampled with 500 *Hz*.

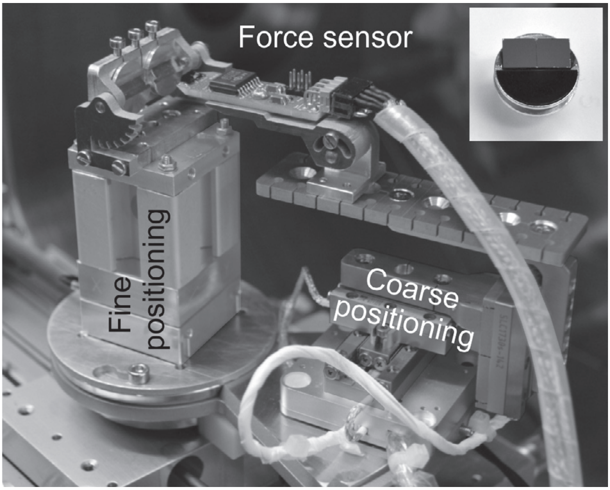

Figure 1. Overview of the customised microrobotic system *PS-AMiR*. A coarse positioning module (right), carrying the sensor, and a fine positioning module (left), performing the actual measurement movement, were chosen. In the top-right corner a detail image of the modified stub can be seen.

Figure 2 shows the schematic scene with the sensor in contact with the fibre. The directly affected fibre length is 50 μm because of the sensor tip. The vision axis of the SEM is in the same direction as the longitudinal axis of the fibre. Before the testing was started, the sensor was tele-operatedly placed close to the fibre, as the large image in Figure 3 shows. Now the fibre was again tele-operatedly guided by the sensor tip against the silicon substrate until these came in close contact. However, this was somewhat difficult as the operator has to take care not let the fibre slip away from under the sensor tip, what it would do due to its intrinsic stiffness. Additionally, the upper face, which is visible with the SEM, needs to be in plane with the fibre cross-section. Therefore, also height differences need to be leveled. The resulting position (as schematically shown in Figure 2) was used as a hold or parking position later on, see also the detail images in Figure 3. The *OFFIS Automation Toolbox* was then used to program and execute the testing sequence. In the beginning, the automation system performed one initial compression (only loading) to determine the maximum travel at a given sensor limit. This is done to avoid sensor overload in the subsequent measurements. Afterwards, the automation system starts the compressibility measurement cycles. Every cycle consists of a compression phase (or loading curve, upper curve in the following Figures in Section 3) in which the nano-positioning module is driven with a pre-defined speed towards the sample. Here, the compression speed was set to 5 $\mu m/s$ (sample: Pine 1), or 10 $\mu m/s$ (sample:

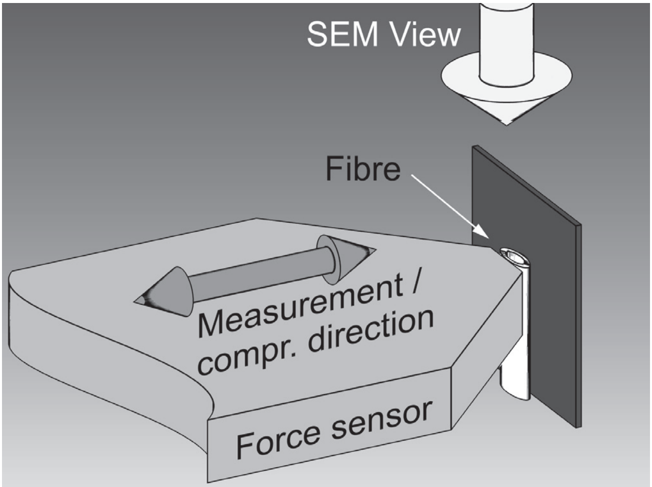

Figure 2. Model of the scene. The SEM can image the cross-section of the tested fibre because the stub is tilted by 90º in both cases, compressibility measurement and periodic compression. The compression takes place in the transverse fibre direction.

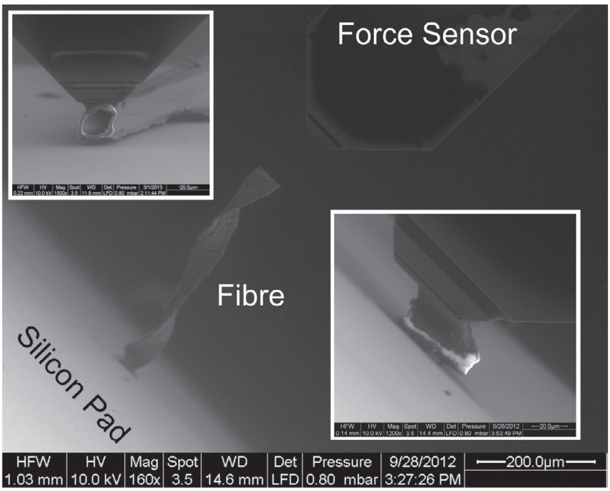

Figure 3. Scanning electron microscopy image of the compression testing. The large and lower right image show the pine fibre. In the upper left corner the virgin earlywood spruce fibre can be seen.

Pine 2 and spruce samples) respectively. After reaching the maximum force or maximum travel the pressure is held for 0.5 *s* before the unloading phase begins. This loading and unloading is performed as often as was entered beforehand by the operator. In this case four to six measurement cycles were performed per sample. Between the cycles another pause of 0.5 *s* is maintained.

2.3 Microrobotic Setup for Artificial Hornification

For the artificial hardening treatment of single fibres, a stick-slip actuatorbased micro-force generator is proposed, as formerly reported by [5].

Figure 4 shows the schematic setup of the micro-force generator. The so-called runner or slide in the form of a rod, tube, or half-tube is guided and supported by four piezoelectric actuators. The piezo-actuators are fabricated out of piezoceramic plates PZT-5H with a thickness of $500\mu m$. The actuators are arranged with an angle of ninety degrees to each other and glued on one of the inner sides of the device's housing. This arrangement proves practical to guide the runner, since it satisfies the kinetic constraint condition, namely the translational movement of the runner. In this design, a ruby hemisphere with a diameter of 1 *mm* is glued onto two segments of piezoceramics and each segment can be controlled separately. With an anti-symmetrical applied control voltage (saw tooth), a partial rotation of the ruby hemisphere is achieved. By oscillating the hemisphere forth and back with different speeds respectively, two phases during one cycle occur. A *slip phase*, where the hemisphere slips through without moving the runner, and a *stick phase* in which the runner sticks to the hemisphere due to friction and other principles [15]. Synchronous rotations of the four ruby hemispheres are transformed to the translational motion of the runner through the contacts between the runner's surfaces and the ruby hemispheres of the actuators. Therefore, the drive is controlled by a saw-tooth signal. The maximal signal's amplitude is ±150 *V* with

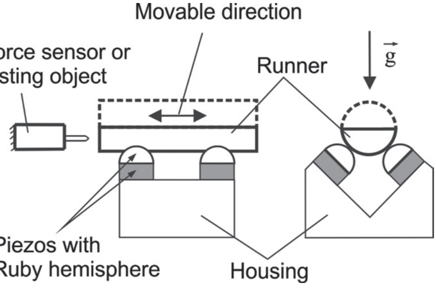

Figure 4. Schematic of the Slip-Stick-Drive (SSD). The weight of the runner is the only force acting against the movement of the piezoelectric controlled ruby hemispheres.

a typical slewrate of 150 $V/\mu s$. The maximal amplitude will be considered to be 100%. The frequency, slewrate, and amplitude of the control signal can be regulated. The preload, responsible for the normal force in the contact zone between the ruby hemispheres and the runner's surfaces, is created by the weight of the runner itself and has also a direct impact on the achievable force [4].

The method for the μ-scale force generator using stick-slip drives (SSDs) is based on the idea that the runner of a SSD runs against an obstacle. In this very moment a force appears. This force can be controlled by the control signal's amplitude of the SSD. Thus, after a calibration process, the dependency of the amplitude on the generated force is known and can be applied. Figure 5 shows the relations between the generated force and the control signal (amplitude). At the time of contact, the drive changes its function from a positioner to a force generator. The generated force is calibrated by a force sensor from Femtotools which offers the measurement in range of several μN to 2 mN. The main advantage of this method is that no additional sensor is needed miniaturised and the stick-slip drives can be miniaturized very well offering wide range of application in the field of micro and nanorobotics. Furthermore, due to the characteristics of stick-slip principle the generated force is in fact not continuous force but periodic force, as Figure 5a) suggests. The period of the generated force depends on the frequency of the control signal.

Therefore, to achieve periodic loading of a single fibre in relatively short time SSD offers itself as a useful technique. Figure 5 shows the steadiness and range of available forces for one possible runner (weight: 292 mg). Figure 5a) shows the result of measurements of generated force at amplitude of 50%. At about 2 s the runner reaches the head of force sensor. Then the force is generated and measured.

Figure 5b) shows the dependency of the generated force on control amplitude of input signal. At first, the force increases proportionally with the rise of amplitude. Eventually, the saturation status is obtained. By using different runners

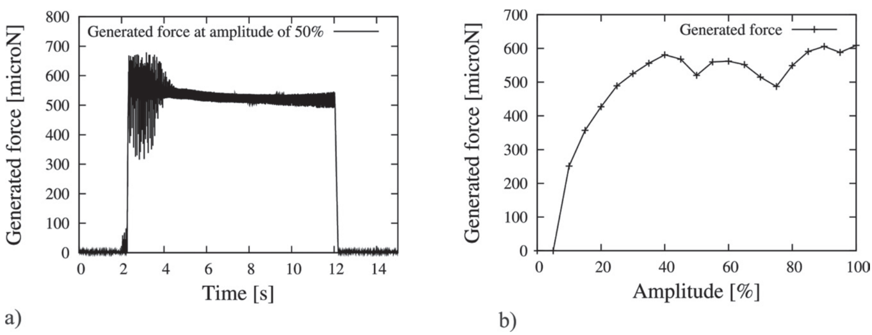

Figure 5. Force generation at a fixed control amplitude (a) and the generated force over different control amplitudes (b). The weight of the runner was not changed.

and changing the control amplitude of the input signal, a virtually arbitrary generated force in range of several tens of *μN* to 2 *mN* can be achieved.

In this work we use SSD to generate periodic forces preferably in range of hundreds of *μN*, which is the same range the force sensor uses during the compression measurement. When the runner of SSD runs in contact with the fibres, they will be compressed with a given force. Due to the sawtooth signal one signal period corresponds to one step, i.e. the number of compression steps can be controlled. With a rather slow driving frequency of 1 *kHz* the runner drives against the fibres. Only the virgin spruce fibres are compressed this way as the biggest effect is expected with those than with the already processed (pulped) pine fibres. Both fibres are compressed with the same runner, i.e. the same basic force of ca. 550 *mN*. However, one fibre (Spruce 1a) is compressed with 100,000 steps whereas the other fibre (Spruce 2b) is compressed with 1 million steps. The other halves of the fibres (Spruce 1b and Spruce 2a) are not compressed and measured in the SEM only for reference. Thus it is suggested that the mechanical hardening can be simulated with this device. Figure 6 shows the realised setup under light microscopy, which in turn bases again on the PS-AMiR.

The previous testing procedure is part of these periodic compression tests. When the fibres are placed on the modified stub they are tested according to the protocol above. After that they are treated in the force generation apparatus and eventually tested again in the SEM. So, there is a transfer of the earlywood spruce fibres from the low vacuum atmosphere in the SEM to the SSD compression device at ambient conditions and back into the SEM for the final compressibility test.

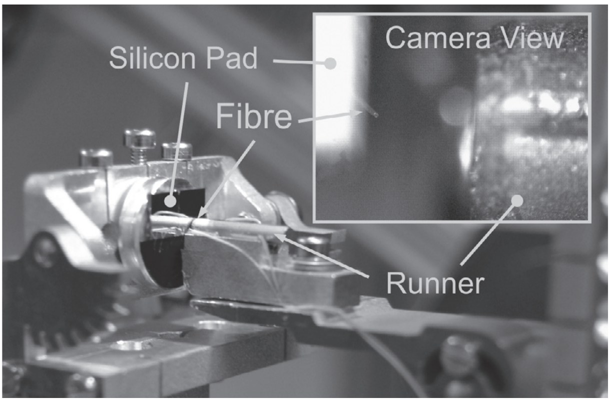

Figure 6. A slip-stick drive is used as a compression setup for fibres to simulate hornification effects. The runner is also equipped with a silicon disc to achieve a very flat compression surface.

3 RESULTS

Three sets of compression measurements were made: (i) a totally collapsed pine fibre (Pine 1), (ii) a nearly collapsed pine fibre (Pine 2), and (iii) two earlywood spruce fibres (Spruce 1a and Spruce 2b) which were also periodically compressed with the SSD, with 100k and 1000k times, respectively. From the force-distance curves, recorded during testing and with ca. 1000 to 5500 data points each, the compression of the fibres can be clearly shown. Depending on the fibre, a certain force was necessary to bend the fibres towards the silicon background. For the pine fibres this bending forces were around 30 . . . 100μN, whereas the virgin spruce fibres this force was generally around 500μN. All measurements were smoothed by a moving average over 20 data points for better visualisation.

The SEM images allow the determination of the fibre cross-sectional features, such as fibre wall thickness or the lumen size. However, other morphological, e.g. microfibril angle, data was not obtained at this point.

3.1 Pine fibres

From Figure 7 the typical course can be determined. In the beginning the curve starts very flat, has an intermediate slope in the middle and increases rapidly when the fibre is completely pressed on the silicon background and only the fibre walls are compressed. Four full cycles (loading and un-loading) were measured and a significant decrease in the loading curves can be seen. This decrease is gradually reduced. The un-loading curves, however, follow nearly the same path.

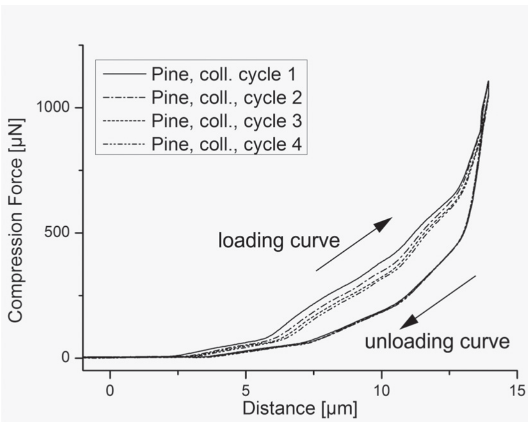

Figure 7. Pine 1 – A collapsed pine fibre.

Figure 8 shows the results of a set of compression cycles on the the second pine fibre (Pine 2), also imaged in Figure 3. With every additional cycle the necessary compression forces decrease, as to be seen in the small inlayed diagram. The maximum achieved force dropped in this measurement from ca. $1096\mu N$ to ca. $1029\mu N$. As the maximum travel was determined by the first sensor approach, all other curves stop at the same distance. However, this behaviour shows a certain amount of fatigue when compressed. Every cycle needs ca. $10 \ldots 20s$ for the loading and the same time for the unloading phase at a speed of $10\mu m/s$, or $5\mu m/s$ respectively. Furthermore, the results indicate that after a certain amount of cycles the reduction of force comes to a halt. For the six cycles measured this saturation was obviously still not achieved.

In this set of experiments for the second pine fibre (Pine 2) the same fibre was measured four times, at the same spot and every time with six cycles. The parking position was not changed during these measurements. When the results are compared between these measurements the general trend of decreasing maximum force from earlier to later cycles, as mentioned above, can be confirmed—even on the same fibre; compare Figure 8. However, with every measurement the necessary force to compress the fibre decreases, as if the fibre becomes less stiff and does not fully relax after compression. Therefore, longer travels for the later measurements and higher forces become possible, as can be seen in Figure 9. Additionally, the later measurements and their cycles show in general also a

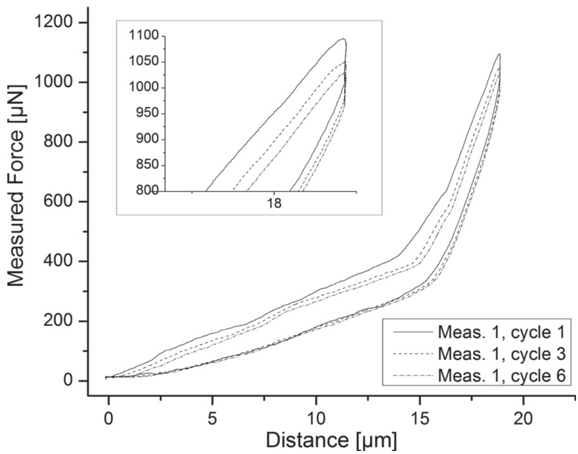

Figure 8. Pine 2 – Decreasing maximum force with increasing number of cycles. Not all cycles are shown here to emphasise the drop in force, although the characteristic slope remains the same.

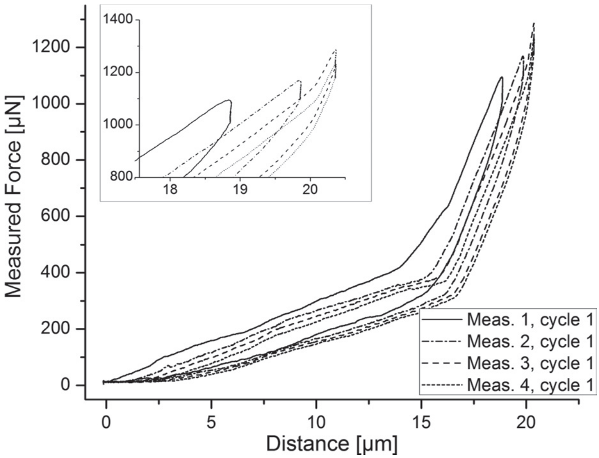

Figure 9. Pine 2 – Four measurements on the same fibre, all with six cycles. However, here are just the first cycles of all measurements shown.

smaller enclosed area, which can be seen as a reduced amount of energy necessary to compress the fibre. The plateau that forms at ca. $300 \mu N$ can be seen as the necessary force to push the fibre flat to the substrate, and is rather constant.

3.2 Spruce fibres

When looking into the spruce fibres in Figure 10 and Figure 11 no big difference can be seen. The same trend as with the pine fibres cannot be directly recognised. The fibres needed already a rather high force to bend them towards the silicon substrate. The shift in the curves results from the relocation of the sensor: after applying the periodic compression with the slip-stick drives another parking position was introduced when the samples were transferred back into the SEM for the control measurements. However, due to the intrinsic stiffness of the fibres they did not twist, so that the measurement direction and the sensor-fibre/fibre-substrate interfaces were the same for the measurements before and after the artificial hardening.

The maximum force, however, does not remain the same for the different cycles for the respective fibres, Spruce 1 and Spruce 2. A slight change can be recognised as Table 1 shows. This change is additionally not as big as with the pine fibres. When the data of the spruce fibres is analysed for the slope of the un-loading curve, see Figure 12, one can recognise another change. In contrast to the slope in the fibre with 100k compression, which did not change significantly ($441 \pm 3 \mu N/\mu m$), the change for the fibre with 1 Million periodic compressions

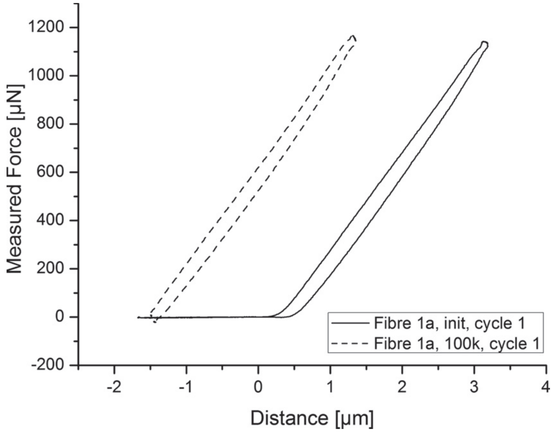

Figure 10. Spruce 1a – Compression measurement of the fibre before the artificial hornification (*init*-curve) and after compressing the fibre 100,000 times (*100k*). Only the first cycle is shown here.

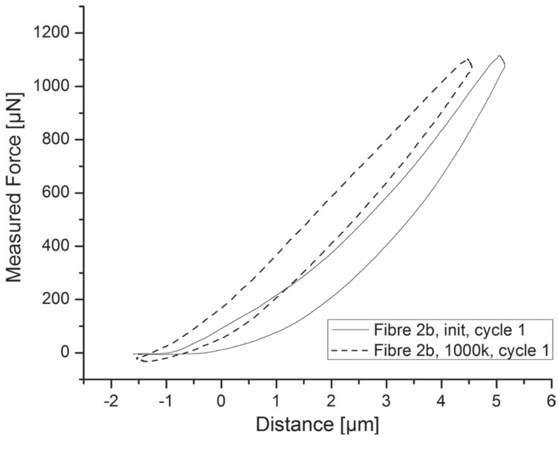

Figure 11. Spruce 2b – Compression measurement of the fibre before the artificial hornification (*init*-curve) and after periodically compressing the fibre 1 Million times (*1000k*-curve).

changed significantly: It dropped from initially $235 \pm 3\mu N/\mu m$ to $222 \pm 1\mu N/\mu m$ after the compression. Additionally, as the initial slope variation suggests, there is also a change during the initial measurements with a trend to higher values for later cycles.

Table 1. Maximum forces of the spruce fibre measurements

Cycle num.	*Spruce 1a init Force/µN*	*Spruce 1a 100k Force/µN*
Cycle 1	1143	1168
Cycle 2	1136	1153
Cycle 3	1131	1146
Cycle 4	1126	1140
Cycle num.	*Spruce 2b init Force/µN*	*Spruce 2b 1000k Force/µN*
Cycle 1	1117	1104
Cycle 2	1095	1093
Cycle 3	1080	1084
Cycle 4	1072	1076

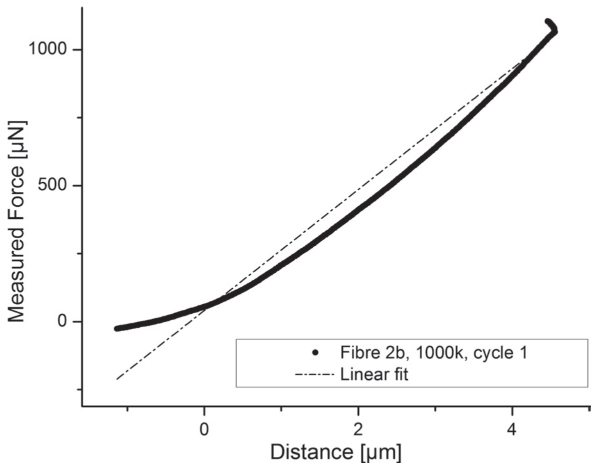

Figure 12. Linear fit of the un-loading curve of Spruce fibre 2b after the artificial hornification.

4 DISCUSSION

Introducing micro and nanorobotic tools in the fibre research proved to be useful as it becomes possible to work on single fibre level or even smaller. Performing such experiments requires, however, a suitable visualisation tool. The SEM proved to be useful here, especially a SEM with low vacuum or environmental

SEM (ESEM) mode allows visualisation without significantly influencing the mechanical properties by a coating. However, temperature control of the specimens will increase the reliability of these *in-situ* testing devices.

Currently available micro- and nanorobotic tools are useful but not yet easy to handle. It either needs a skilled tele-operator or a sophisticated automation system. The OFFIS Automation Toolbox proved to be a helpful piece of software as it allows simultaneously automation and tele-control of the different components with a game pad. The approaching and testing sequences were easily scripted in Python™ and reliable.

Regarding the force generating device, it was as well controlled by the OFFIS Automation Toolbox, and therewith easy to use. However, having the results from Section 3.2 in mind, there is need in optimization. The influence on the fibres was not as large as expected. This might be due to the smaller force when the drive has reached the obstacle. Figure 5a) shows the ripple around the force of ca. $550\mu N$, which will have been the periodic force exerted on the fibre. Only with a huge amount of cycles this smaller force produces a significant effect. The level of the generated force needs therefore to be varied, which can be done by changing the control amplitude of the input signal and the normal force. In this case, the normal force could be changed by using runners with different weights.

Concerning the fibre's response to the mechanical treatment more investigations are necessary to justify the term hornification. However, the general trend of the earlywood spruce fibre to stiffen could be recognised for the two tested fibres, as it is proposed by [8]. Future experiments need to take also the wetting and drying into account. With the proposed setup these could be integrated as well. In the low vacuum of the SEM a water atmosphere is created. Together with a temperature control of the sample also the relative humidity can be controlled. Therefore, a suitable combined measurement setup could include compression testing, periodic compression, a drying/rewetting part, together with an indication device for hornification.

The compression measurement inside the SEM allows the visualisation of the fibre cross-section as seen in Figure 3 during testing. The results, too, are promising. The reduction in the maximum force with the pine fibres suggests a change in the fibre structural mechanical properties. Especially when comparing Figures 7 and 8 similar effects can be recognised. As the force sensor was still operated in the nominal region and the influence of sensor creep can, according to Figure 7, if not excluded but seen with reduced impact on the measurement. However, slower testing speeds (e.g. $1\mu m/s$) and higher sampling rates (e.g. $1\ kHz$) can be tested to increase the measurements reliability. The recorded data for one fibre is enough to be statistically relevant. However, several hundred fibres need to be tested to obtain statistical relevant data for a species of fibres. Automating the sample preparation and testing are essential for future tests. Furthermore, additional morphological data (i.e. microfibril angle and cell wall thickness) need to be gathered for detailed understanding and modeling.

5 CONCLUSION AND OUTLOOK

Two useful microrobotic setups were presented to perform (i) single fibre compression measurements in transverse fibre direction inside the SEM and (ii) to periodically compress single fibres. The resulting curves show a decrease in stiffness for increasing compression cycles (mechanical wear) and increasing number of artificially compressions. Especially for the already processed (i.e. pulped) pine fibres. Fresh fibres, however, respond with a partial hardening (Table 1, Spruce 1a – 100k). This effect can be seen as a mechanically induced hardening. Future activities need to include more fibres, virgin and processed, and possibly different species to compare and evaluate the findings. The current results suggest that there is an initial hardening with fibres that still contain lignin (the spruce fibres) compared to fibres with a very low lignin content (the tested pine fibres), which in contrast get weaker and loose their strength. This history can now be quantified by the micro and nanorobotic systems.

Further automation of the experiments for autonomous testing of several fibres in a row will help to achieve statistically relevant data. Different tasks in this respect present themselves from the made experiments. First, developing a cross-section recognition and sensor guiding method in the OFFIS Automation Toolbox vision system will allow the automatic approach of the fibre. This is also necessary to automatically locate the fibres in the SEM and can deliver cell wall thickness and the lumen size simultaneously. Second, developing push strategies to press the fibre with the sensor tip towards the silicon tiles. During tele-operated movements, the operator can account for fibre slipping on the sensor tip. However, the automation system needs to be trained to do so. With these two advancements several fibres can be tested in a row and only the sample holder will limit the number of samples. This development is best accompanied by an automated sample preparation system, as described by Saketi *et al.* [17]. Another improvement will be controlling the sample temperature by a heating/cooling system inside the SEM.

Regarding the force generation device, a more detailed investigation is necessary. Especially the difference between the two possible modes of compression: (i) driving the runner only once against the target and compress only with the SSD's control signal (as done in this study), or (ii) continuously move the runner against and away from the fibre. Additionally, the influence of humidity can be included in the investigation as well by transferring this setup into a climate chamber.

Overall, localised manipulation and characterisation of single fibres becomes possible with micro- and nanorobotic tools. This appears to be an ideal expansion to the existing single fibre methods. It is expected that with such tools the ultrastructure of single fibres can be assessed in the near future.

6 ACKNOWLEDGEMENTS

Parts of the presented work were carried out in the ERA-NET WoodWisdom project *PowerBonds*. The authors gratefully acknowledge the discussions with Michaela Eder from Max Planck Institute of Colloids and Interfaces (Potsdam, Germany) and for supplying the virgin Spruce fibres.

REFERENCES

1. R.B. Adusumalli, R. Raghavan, R. Ghisleni, T. Zimmermann, J. Michler. Deformation and failure mechanism of secondary cell wall in Spruce late wood. *Appl. Phys. A* 100(**2**):447–452, 2010.
2. I. Burgert, K. Frühmann, J. Keckes, P. Fratzl, S. Stanzl-Tschegg. Microtensile Testing of Wood Fibers Combined with Video Extensometry for Efficient Strain Detection. *Holzforschung* **57**:661–664, 2003.
3. I. Burgert, M. Eder, K. Frühmann, J. Keckes, P. Fratzl, S. Stanzl-Tschegg. Properties of chemically and mechanically isolated fibres of spruce (*Picea abies* [L.] Karst.). *Holzforschung* **59**:354–357, 2005.
4. C. Edeler. Dynamic-mechanical Analysis of Piezoactuators for mobile Nanorobots. In proc. *ACTUATORS 2010*, Bremen, Germany, 2010.
5. C. Edeler. Modellierung und Validierung der Krafterzeugung mit StickSlip-Antrieben für nanorobotische Anwendungen, Doctoral thesis, 1. Ed., Department for Information Technology, University of Oldenburg, 2011.
6. M. Eder, O. Arnould, J.W.C. Dunlop, J. Hornatowska, Lennart Salmén. Experimental micromechanical characterisation of wood cell walls. *Wood Sci. Technol.* **47**:163–182, 2013.
7. J.M.B. Fernandes Diniz, M.H. Gil, J.A.A.M. Castro. Hornification – its origin and interpretation in wood pulps. *Wood Sci. Technol.* **37**:489–494, 2004.
8. M.A. Hubbe, R.A. Venditti, O.J. Rojas. What happens to cellulosic fibers during papermaking and recycling? A review. *BioResources* 2(**4**):739–788, 2007.
9. B.A. Jayne. Mechanical properties of wood fibers. *Tappi* 42(**6**), pp. 461–467, 1959.
10. K.L. Kato and R.E. Cameron. A Review of the Relationship Between Thermally-Accelerated Ageing of Paper and Hornification. *Cellulose* 6(**1**):23–40, 1999.
11. P.C. Kersavage. A system for automatically recording the leadelongation characteristics of single wood fibers under controlled relative humidity conditions. *Bulletin – Agricultural experiment station*, No. 790, Pennsylvania State University, University Park, 1973.

12. M. Mikczinski, M. Bartenwerfer, P. Saketi, S. Heinemann, R. Passas, P. Kallio and S. Fatikow. Towards Automated Manipulation and Characterisation of Paper-making Fibres and its Components. In **Fine Structure of Papermaking Fibres** (ed. P. Ander), Uppsala, Sweden, Swedish University of Agricultural Sciences, pp. 163–178, 2011.
13. A.-M. Olsson, L. Salmén, M. Eder, I. Burgert. Mechano-sorptive creep in wood fibres. *Wood Sci. Technol.* **41**:59–67, 2007.
14. D.H. Page, F. El-Hosseiny, K. Winkler. Behaviour of single wood fibres under axial tensile strain. *Nature* 229:252–253, 1971.
15. V.L. Popov. Friction Under the Influence of Ultrasonic Vibrations. Ch. 18 in **Contact Mechanics and Friction – Physical Principles and Applications** (ed. V.L. Popov), Springer, Berlin, 2010.
16. P. Saketi, A. Treimanis, P. Fardim, P. Ronkanen, P. Kallio. Microrobotic platform for manipulation and flexibility measurement of individual paper fibers. Proc. on *IEEE/RSJ International Conference on Intelligent Robots and Systems* (IROS), Taipei, China, October 18–22, pp. 57625767, 2010.
17. P. Saketi, M. von Essen, M. Mikczinski, S. Heinemann, S. Fatikow, P. Kallio. A flexible microrobotic platform for handling microscale specimens of fibrous materials for microscopic studies. *J. Microscopy* 248(**2**), pp. 163–171, 2012.
18. P.M. Wild, J.W. Provan, R. Guin, S. Pop. The effects of cyclic axial loading of single wood pulp fibers at elevated temperature and humidity. *Tappi* 82(**4**), pp. 209–215, 1999.
19. D. Yan and K. Li. Conformability of wood fiber surface determined by AFM indentation. *J. Mater. Sci.* 48(**1**):322–331, 2013.
20. X. Zhang, Q. Zhao, S. Wang, R. Trejo, E. Lara-Curzio, G. Du. Characterizing strength and fracture of wood cell wall through uniaxial microcompression test. *Composites A* 41(**5**):632–638, 2010.

Transcription of Discussion

ASSESSING TRANSVERSE FIBRE PROPERTIES: FIBRE COMPRESSION AND ARTIFICIAL HORNIFICATION BY PERIODIC COMPRESSION

Manuel Mikczinski,[1] *Ha Xuan Nguyen,*[2] *and Sergej Fatikow*[1,2]

[1] OFFIS – Institute for Information Technology, Division Health, Group Automated Nanohandling, Escherweg 2, D- 26121 Oldenburg, Germany
[2] University of Oldenburg, Division Microrobotics and Control Engineering, D-26111 Oldenburg, Germany

Ulrich Hirn Graz University of Technology.

First I would like to point out that there has been work on transverse compression by a Canadian group at the end of the 90's and published in the Journal of Pulp and Paper Science[1]. It might be interesting to compare your results to theirs. Secondly, I would like to point out that we have measured transverse properties using atomic force microscopy. It has recently appeared in Holzforschung[2] and I totally agree with you that it is very, very important to control humidity. We have measured a fourfold decrease in indentation hardness and effective elastic modulus over a span from 5 to 80% relative humidity.

Manuel Mikczinski

Actually, I would like to comment on your AFM testing. Of course, it is possible to characterise this material with an indentation hardness procedure, but the

[1]J.A. Dunford and P.M. Wild, "Cyclic transverse compression of single wood-pulp fibres", Journal of Pulp and Paper Science, April 2002, Vol. 28(4).
[2]C. Ganser, U. Hirn, S. Rohm, R. Schennach and C. Teichert, "AFM nanoindentation of pulp fibres and thin cellulose films at varying relative humidity", Holzforschung. Pages 1–8, May 2013.

difference to our technique is that we compress the whole fibre section. So it might be complementary and it would be nice to see how the results correlate in this case.

Ulrich Hirn

I totally agree with you, because the difference we see to this older study by the Canadian group is that, on the surface, the material seems to be softer than on the inside, so it is definitely complementary.

Mikael Magnusson KTH

Could you go back to the slide with the first force displacement curve you showed (figure 7 in the text). Was this the wood fibre or the pulp fibre?

Manuel Mikczinski

This is the bleached softwood kraft pulp fibre.

Mikael Magnusson

Do you know the dimensions, like the height or the radius of the cross section?

Manuel Mikczinski

When we go to this slide, it is fairly easy to see. So you can see the sensor tip is approximately 50 μm in width, so the fibre's in the range of 40 μm approximately.

Mikael Magnusson

You are in the range of 15 μm displacement, so I thought that you were crushing the fibre, but it was a big fibre.

Manuel Mikczinski

I think we will partially do this because, as you see here, this is our parking position and when you correlate the distance between this shadow on the substrate here and this sensor tip corner here, you will end up with something like 12 μm. So it is already pretty good.

Doug Coffin Miami University

Take the slide where you show the load goes down each time. Is it just a matter that you are going to the same end displacement each time? You are getting permanent deformation so it is not reaching the same load level, because you are shifting where you start to load the fibre? And when you say the fibres are getting weaker, have you tested them all the way to failure? Do you know you are actually weakening the fibres or are you just getting again some kind of permanent deformation? With each cycle, you are not allowing recovery so you have a viscous hardening. How do you separate all that out?

Manuel Mikczinski

We have not sorted that out yet. We were focusing firstly on the method, so these are the first results of those methods. But taking also different effects like plastic deformation or viscous hardening of the fibre into account, this will be one of the next steps as well. As we are not fibre experts, we need to figure out what is happening there in the compression zone as well. There is a common understanding that there must be several effects on the fibre wall, like shifts between the fibre wall layers or the fibre wall settling, but we have not sorted that out yet.

Wolfgang Bauer Graz University of Technology (from the chair)

Did you observe any delamination in the fibre wall between the fibre wall layers when you are compressing the fibres?

Manuel Mikczinski

Not yet. The image resolution was not good enough to see that.

Wolfgang Bauer

Do you have the potential to go up in resolution in the SEM?

Manuel Mikczinski

I hope so. The problem is with all those systems, we need a different working distance. It would be nice to go to the official 10 mm, or even below that, but we need to be careful that we do not run into the cone of the SEM. So it is a bit tricky to really get close to the electron gun cone. If we can make sure that we will not collide with the cone and come closer to it with the system then we should get better image resolution.